Thin Solid Films 517 (2009) 4251–4254

Contents lists available at ScienceDirect

Thin Solid Films

journal homepage: www.elsevier.com/locate/tsf

Characteristic study of atmospheric pressure microplasma jets with various operating conditions

S.J. Kim, T.H. Chung *, S.H. Bae

Department of Physics, Dong-A University, 840 Hadan-dong, Saha-gu, Busan 604-714, Republic of Korea

ARTICLE INFO

Available online 8 February 2009

Keywords:
Atmospheric pressure microplasma jet
Cold plasma source
Non-thermal plasma
Corona discharge
Dielectric barrier discharge (DBD)
Ground ring electrode

ABSTRACT

Non-thermal microplasma jets generated under atmospheric pressure by means of radio-frequency of 13.56 MHz and low-frequency of several tens of kilohertz are characterized. They show several distinct discharge characteristics. Two operation modes of the plasma are observed when the single pin electrode is utilized and separated by the remote ground, and where plasma is sustained between the pin electrode and the ground ring electrode. The electrical characteristic of discharges and various effects of the ground ring electrode are presented. We observe that the emission spectra are dominated by the presence of excited nitrogen, helium, and nitrogen ions. Highly reactive radicals such as hydroxyl (OH) and atomic oxygen are also detected. With the addition of a ground ring electrode, the discharge current and optical emission intensities from the plasma plume are enhanced significantly indicating that the generated plasma is near the glow discharge mode.

1. Introduction

Atmospheric pressure microplasma jets have become hot issues of current low-temperature plasma research because of their immense potentials for material processing and biomedical applications [1]. The microplasma jets generate plasma plumes in open space. Thus, they can be used for direct treatment [2]. They have been operated at an excitation frequency either in the several tens of kilohertz ac range or in the radio-frequency (RF) range [2–5]. Due to various design configurations and operation conditions of microplasma jets, the factors governing the discharges, for instance, heat, charged particle, electric field, chemically active species may be very distinct [6].

The plasma generation in microplasma jets relies mainly on two mechanisms; corona discharge and dielectric barrier discharge (DBD) [7–9]. A corona discharge appears as a luminous glow localized in space around a point tip (or wire) in a highly non-uniform electric field. Dielectric barrier discharges operating at atmospheric pressure are driven by a pulsed or sinusoidal voltage at frequencies from 50 Hz up to several tens of kHz (even up to RF) and at least one of the electrodes has insulating layer. The corona and DBD hybrid discharge system is accessible to generate a glow discharge, and its characteristics can be controlled to suitable condition [10].

In this paper, specially designed microplasma jet devices driven by a 50 kHz ac and 13.56 MHz RF voltages are reported. These devices also utilize the working principles of corona discharge and DBD. For better control of the treatment processes, it is essential to understand the basic physical and chemical properties of the microplasma jet such as electrical characteristics and power deposition, optical emission spectrum, and gas temperature [3,4,10,11].

2. Experimental setup

Fig. 1 shows the schematic illustration of the experimental setup. Fig. 1(a) shows the jet device driven by 50 kHz ac voltage. At the center of the glass tube is a copper wire with a diameter of 0.9 mm and a pencil-shaped tapered end. The power source (FTLab HPSI200) of 50 kHz is applied to the copper wire. The wire was concentric with a T-shaped cylindrical glass tube, which has an inside diameter of 6 mm and an outside diameter of 8 mm. The wire shaft was covered with a polyethylene insulator tube, leaving a length of 4 mm of the wire exposed to gas. The glass tube is filled with helium gas (UHP 99.999%) delivered at a flow rate 3 l/min, controlled by a flow meter (Kofloc RK1600R).

Fig. 1(b) shows the jet device driven by 13.56 MHz RF voltage. The power source (YS E03F) of 13.56 MHz is applied to the tungsten wire through matching network. This flexible hand-held device consists of a tungsten wire (0.3 mm diameter) with sharpened tip, confined in a Perspex tube (7 mm inner diameter). The wire was inserted coaxially in a Perspex tube and it protruded from the stainless steel holder by 1.3 cm. The RF plasma jet device utilizes a combination of a single pin corona discharge with an RF coaxial cylindrical capacitive discharge [4]. The power is monitored using a power meter (DAIWA DP810) connected via dual directional coupler (AR DC2600). Using a digital oscilloscope (LeCroy WS44Xs) the discharge electrical circuit was monitored for the applied voltage through the HV probe (Tektronix P5100) and for the circuit current through the current monitor (Pearson 3972).

* Corresponding author.
E-mail address: thchung@dau.ac.kr (T.H. Chung).

0040-6090/$ – see front matter
doi:10.1016/j.tsf.2009.02.013

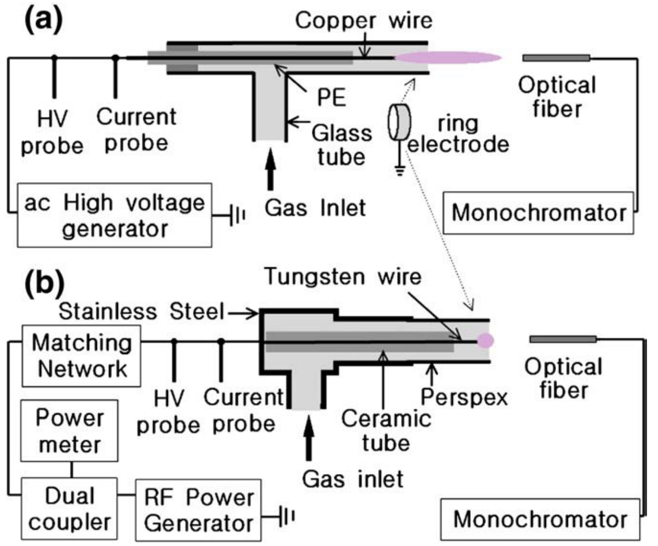

Fig. 1. Schematic of the experimental setup. (a) The LF (50 kHz) microplasma jet and (b) the RF microplasma jet with the diagnostics systems.

To identify reactive species that are generated in the discharge and subsequently expelled with the gas flow, spectra were recorded for emission along the axis of the plasma jet in the range from 300 to 800 nm. The light emitted by the microplasma was focused by means of optical fiber into entrance slit of 0.75 m monochromator (SPEX 1702), equipped with a grating of 1200 grooves per millimeter and slit width of 100 μm. The light was collimated at the exit slit where a photomultiplier tube converted photons into an electric signal.

3. Result and discussions

When helium is injected from the gas inlet and 50 kHz sinusoidal 1.5 kV voltage is applied to the electrode in Fig. 1(a), the homogeneous plasma is generated and a plasma plume reaching length of 5 cm is launched through the end of the tube and in the surrounding air. The plasma has a cylindrical shape. The length of the plasma plume can be adjusted by the gas flow rate and the applied voltage. If the length of the wire electrode exposed to gas is increased to 3.0 cm, the length of the plasma plume reaches up to 6 cm.

The applied voltage and total current traces for the RF plasma jet produced at the input power of 8 W and the gas flow rate of 2 l/min are presented in Fig. 2(a). The RF plasma operates at relatively low voltages and the power consumption ranges at most a few watts [12,13]. Fig. 2(b) shows a current–voltage curve. When the supplied power varies from 5 to 10 W, the applied voltage is in the range of 180–250 V_{rms} and the measured total current is 280–410 mA_{rms}. According to the current–voltage curve, the power dissipated by the plasma can be estimated to be from 0.44 to 0.87 W.

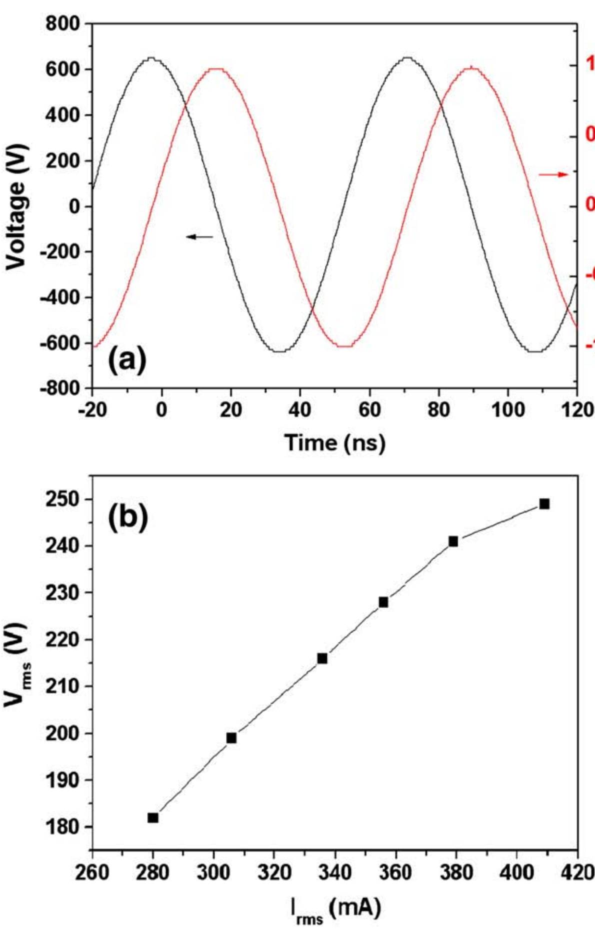

Fig. 2. Applied voltage and total current of the RF plasma jet operating at 2 l/min. (a) the applied voltage and total current trace when the input power is 8 W and (b) the total current versus applied voltage at a frequency of 13.56 MHz.

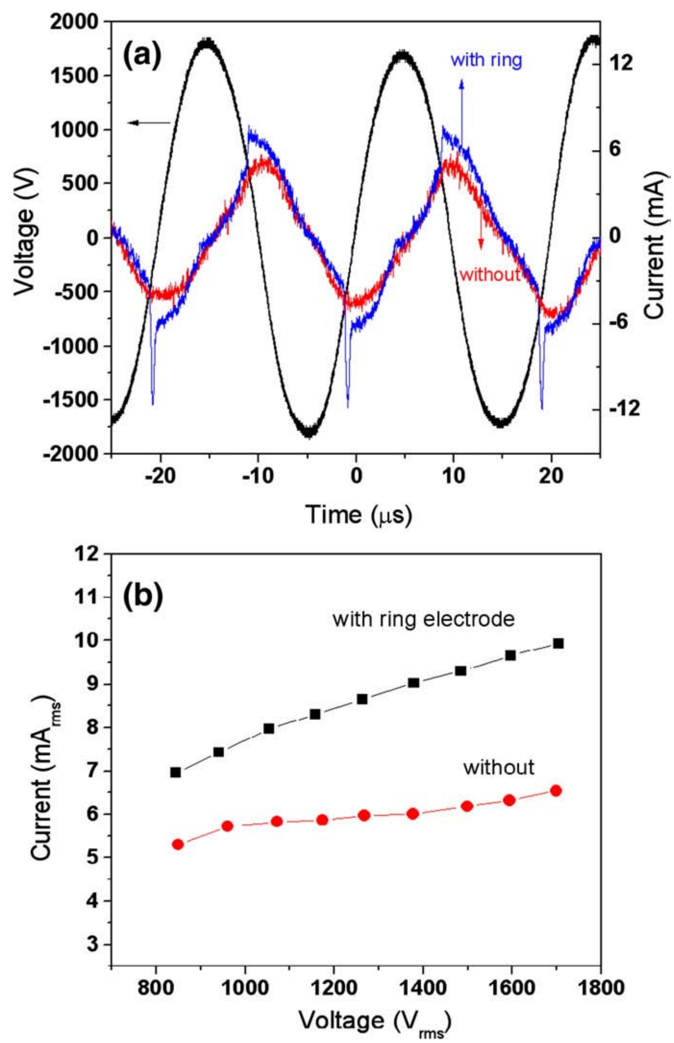

Fig. 3. Applied voltage and total current of the LF plasma jet at a frequency of 50 kHz operating at 3 l/min. (a) the applied voltage and total current traces (*V–I*) with and without the ring electrode. (b) The total current versus applied voltage for two operating modes.

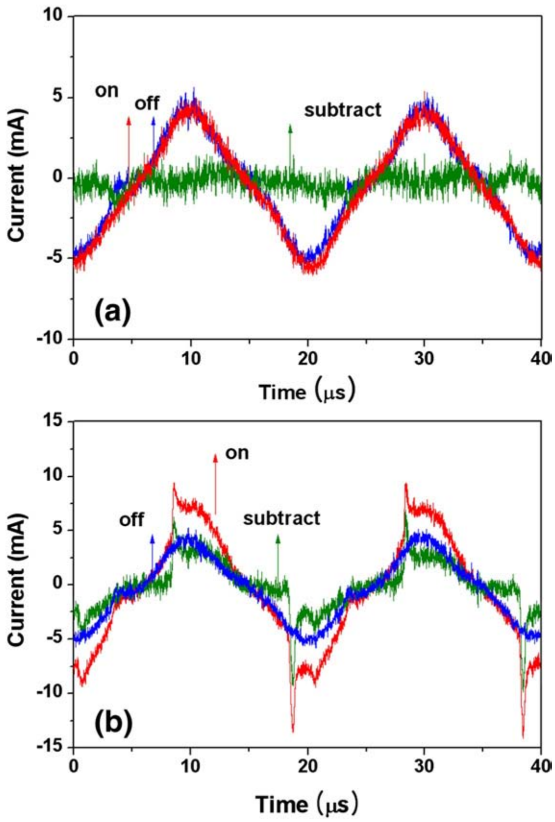

Fig. 4. The traces of total current I_{on} (with plasma on) and I_{off} (with plasma off) for the LF plasma jet (1800 V_{rms}, 3 l/min) at a frequency of 50 kHz without a ground ring electrode (a) and with the ring electrode (b).

Fig. 3(a) shows the applied voltage and total current waveforms of the low frequency (LF) plasma jet operating at 50 kHz and the gas flow rate of 3 l/min. The applied voltage is in the range of 800–1700 V_{rms} and the measured total current is 5.3–6.7 mA_{rms}. According to the current–voltage curve, the power dissipated by the plasma can be estimated to be from 0.3 to 1.5 W. In order to maintain suitable level of the reactive plasma species, the discharge current should not be small. A key issue for atmospheric-pressure microplasma jets is to expand their stability range to larger discharge currents with improved plasma reactivity. When a copper ring, which is attached to the outer surface of the glass tube, serves as a ground electrode, the generated plasma plume has a thicker radius and the plasma discharge current increases. This can be accounted for from that plasma is generated in a pin to dielectric barrier ring electrode structure. When a copper ring serves as a ground electrode, it is clearly observed that the total current is increased. Surface charge accumulated on the dielectric layer beneath the ring during one half period favors the discharge breakdown in the next half. This typically leads to the filamentation of the discharge which is characterized by current spikes of much shorter duration than the ac excitation period. The total current versus the applied voltage for two different operating modes (with and without the ground ring electrode) are presented in Fig. 3(b). The plasma with a ground ring electrode has larger total current amplitude and the difference in the current amplitude between the two modes becomes large as the applied voltage is increased.

Fig. 4 shows the traces of the total current I_{on} (with plasma on) and I_{off} (with plasma off) for the LF plasma jet (1800 V_{rms}, 3 l/min) at a frequency of 50 kHz without ground ring electrode (a) and with the ring electrode (b). The conduction current is obtained by subtracting the displacement current (I_{off}) from the total current (I_{on}). In the case (a), the conduction current is very small and hidden under the waveform of the total current, but with the addition of a ground ring

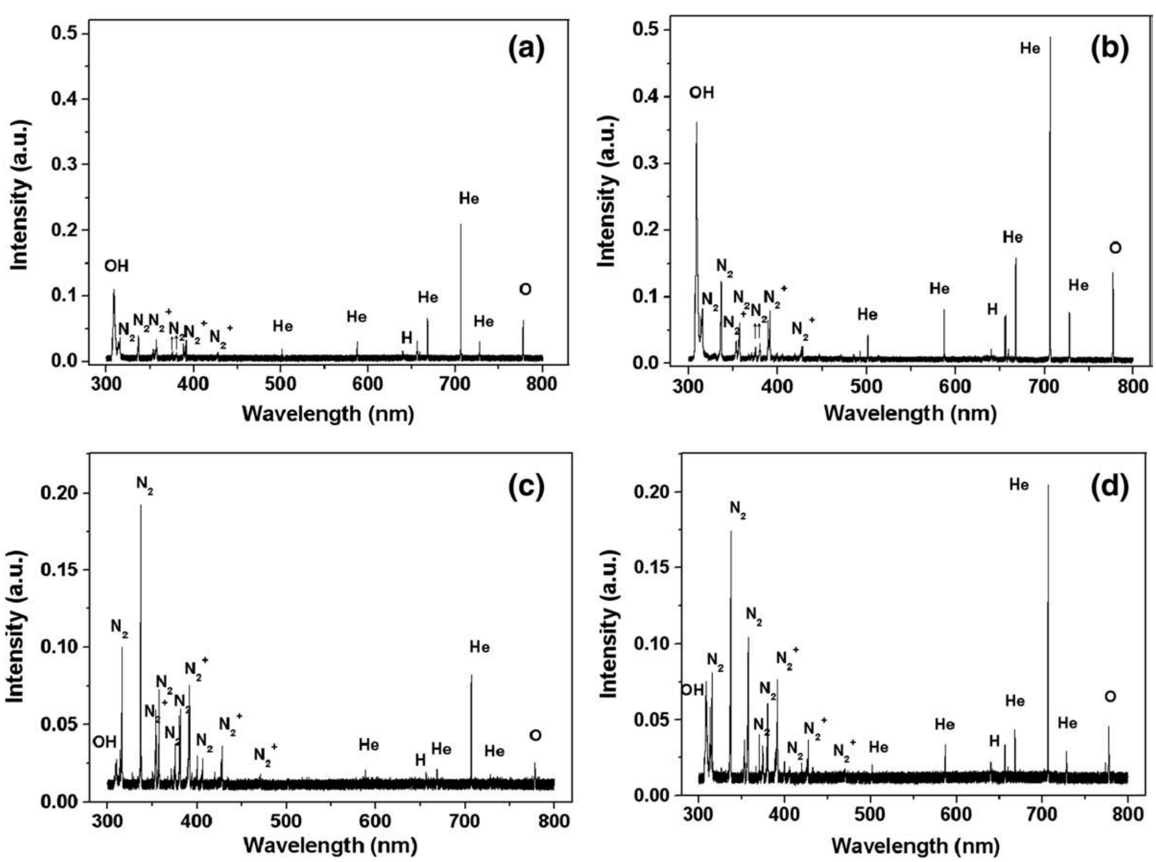

Fig. 5. Emission spectra from 300 nm to 800 nm observed in the RF plasma (8 W, 2 l/min) without a grounded ring electrode (a), with the ring electrode (b), and the LF plasma (1700 V_{rms}, 3 l/min) without (c) and with the ring electrode (d).

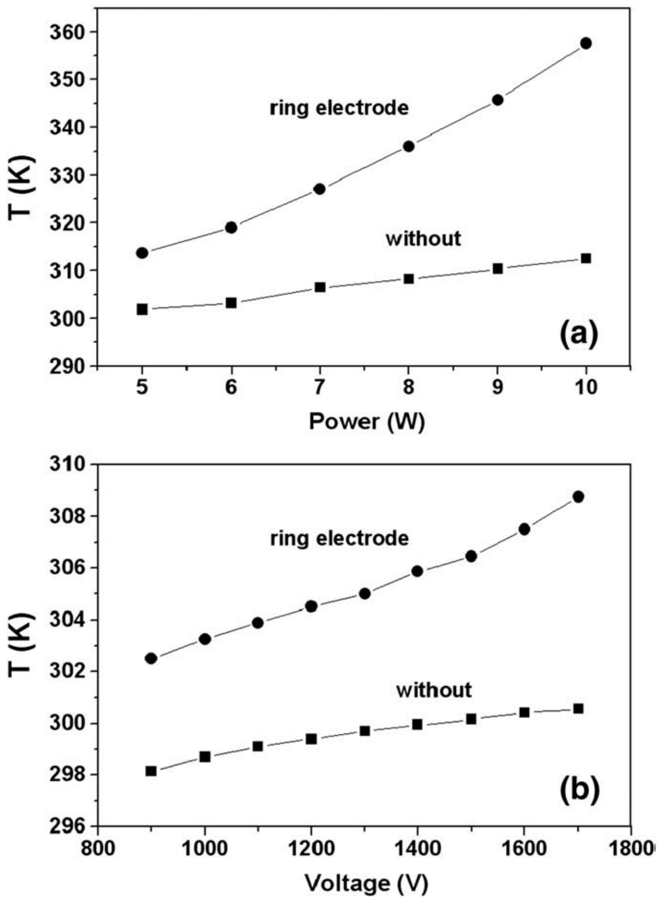

Fig. 6. Measured gas temperature as a function of applied voltage for the RF plasma jet operating at 2 l/min (a) and the LF plasma jet operating at 3 l/min (b) with and without a ground ring electrode.

electrode, as shown in Fig. 4(b), the conduction current becomes significant. In a traditional DBD configuration, it has been demonstrated that the peak conduction current could be dramatically increased [14]. This behavior shows the transition from corona discharge mode to DBD mode.

Fig. 5 shows the emission spectra observed in RF plasma without a grounded ring electrode (a), with the ring electrode (b), and LF plasma without the electrode (c), with the electrode (d). It clearly indicates that excited O, OH, N_2, N_2^+, and He exist in the plasma plume [2,14–17]. The LF plasma emission spectrum shows that there are nitrogen molecular lines as well as a few helium and oxygen atomic lines. The RF plasma emission spectrum indicates that OH and O peaks are enhanced and the N_2 associated peaks become weak compared with the LF spectrum. The RF plasma spectrum has much higher intensity and more helium atomic lines indicating larger plasma density and/or electron temperature [4]. Especially in the RF plasma, with the addition of a ground ring electrode, the optical emission intensities are enhanced significantly indicating that the generated plasma is near the glow discharge mode. The richness of O and OH species makes the microplasma jets suitable for the biomedical applications [18,19].

Fig. 6 shows the measured gas temperature as a function of input power (or applied voltage) for (a) RF and (b) LF plasma jet with and without a ground ring electrode. The gas temperature was measured using a fiber optic temperature sensor (FISO UM14&FOTL-L). The continuous increase in the gas temperature can be seen as the RF power increases. The discharge with a ground ring electrode has larger gas temperature and the increase rate with the power is higher. The LF plasma gas temperature is as low as the room temperature. The increase rate of the gas temperature with applied voltage in LF plasma is much lower than that in the RF plasma.

4. Summary

Compact microplasma jet devices are developed at atmospheric pressure excited at 50 kHz and 13.56 MHz. With the addition of a ground ring electrode, the discharge current and optical emission intensities from the plasma plume are enhanced significantly indicating that the generated plasma is near the glow discharge mode. The richness of O and OH species in the plasma plume makes the microplasma jets suitable for the biomedical applications.

Acknowledgements

This work was supported by the Korea Science and Engineering Foundation under Contract No. 2008-01011. We are grateful to Dr. C. H. Shon of Korea Electrotechnology Research Institute for helpful discussion.

References

[1] M. Laroussi, T. Akan, Plasma Proc. Polym. 4 (2007) 777.
[2] X. Lu, Z. Jiang, Q. Xiong, Z. Tang, X. Hu, Y. Pan, Appl. Phys. Lett. 92 (2008) 081502.
[3] I.E. Kieft, E.P.v.d. Laan, E. Stoffels, New J. Phys. 6 (2004) 149.
[4] D.B. Kim, J.K. Rhee, B. Gweon, S.Y. Moon, W. Choe, Appl. Phys. Lett. 91 (2007) 151502.
[5] N. Puac, Z.L.J. Petrovic, G. Malovic, A. Dordevic, S. Zivkovic, Z. Giba, D. Grubisic, J. Phys. D: Appl. Phys. 39 (2006) 3514.
[6] G. Li, H. Li, L. Wang, S. Wang, H. Zhao, W. Sun, X. Xing, C. Bao, Appl. Phys. Lett. 92 (2008) 221504.
[7] S. Forster, C. Mohr, W. Viol, Surf. Coat. Technol. 200 (2005) 827.
[8] M. Teschke, J. Kedzierski, E.G. Finantu-Dinu, D. Korzec, J. Engemann, IEEE Trans. Plasma Sci. 33 (2005) 310.
[9] A. Fridman, A. Chirokov, A. Gutsol, J. Phys. D: Appl. Phys. 38 (2005) R1.
[10] D.B. Kim, J.K. Rhee, S.Y. Moon, W. Choe, Appl. Phys. Lett. 89 (2006) 061502.
[11] E. Stoffels, R.E.J. Sladek, I.E. Kieft, H. Kersten, R. Wiese, Plasma Phys. Control. Fusion 46 (2004) B167.
[12] E. Stoffels, I.E. Kieft, R.E.J. Sladek, L.J.M.v.d. Bedem, E.P.v.d. Laan, M. Steinbuch, Plasma Sources Sci. Technol. 15 (2006) S169.
[13] W.J.M. Brok, M.D. Bowden, J.v. Dijk, J.J.A.M.v.d. Mullen, G.M.W. Kroesen, J. Appl. Phys. 98 (2005) 013302.
[14] X. Lu, Z. Jiang, Q. Xiong, Z. Tang, Y. Pan, Appl. Phys. Lett. 92 (2008) 151504.
[15] G.H. Marlon, V.P.U. Carlos, C.H. Rafael, Plasma Sources Sci. Technol. 12 (2003) 165.
[16] J.L. Walsh, J.J. Shi, M.G. Kong, Appl. Phys. Lett. 88 (2006) 171501.
[17] M. Laroussi, X. Lu, Appl. Phys. Lett. 87 (2005) 113902.
[18] J.F. Kolb, A.A.H. Mohamed, R.O. Price, R.J. Swanson, A. Bowman, R.L. Chiavarini, M. Stacey, K.H. Schoenbach, Appl. Phys. Lett. 92 (2008) 241501.
[19] J. Goree, B. Liu, D. Drake, E. Stoffels, IEEE Trans. Plasma Sci. 34 (2006) 1317.